

# Borromean nuclei ${}^6\text{He}$ and ${}^8\text{He}$ elastic scattering with heavy targets at near-barrier energies

**Ángel-Miguel Sánchez-Benítez<sup>1</sup>, Gloria Marquínez-Durán<sup>1</sup>,  
Ismael Martel<sup>1</sup>, Krzysztof Rusek<sup>2</sup>, Nicholas Keeley<sup>3</sup>, Kirby  
Kemper<sup>4</sup>, E587S Collaboration**

***Colloque GANIL 2017  
Amboise***

- (1) University of Huelva, Spain**
- (2) Heavy Ion Laboratory, Poland**
- (3) National Centre for Nuclear Physics, Poland**
- (4) Florida State University**



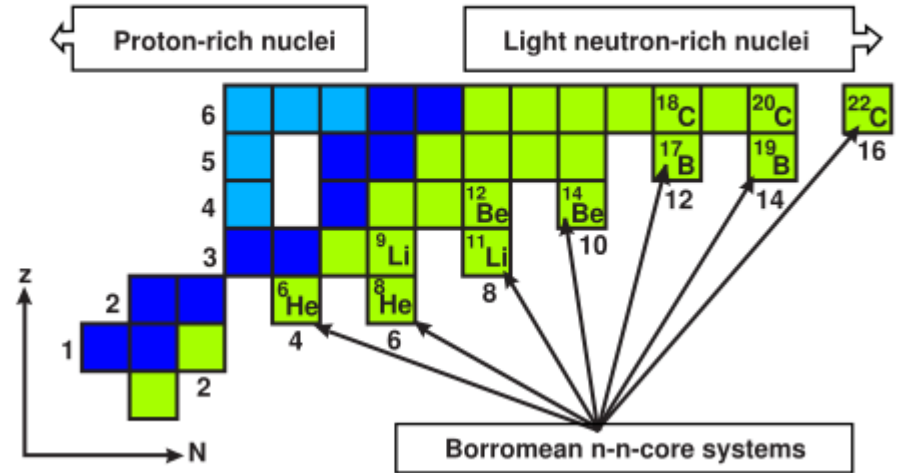
# Outline

- .- Introduction
  - .- Similarities and differences between  $^{6,8}\text{He}$  isotopes
  - .- Expected behavior of the system  $^8\text{He}+^{208}\text{Pb}$  in collisions at barrier energies
- .- Experimental setup for the experiment E587S @ GANIL
- .- Comparison of experimental differential elastic cross sections
  - .- Long range absorption
  - .- Neutron(s) stripping

# Introduction: ${}^{6,8}\text{He}$ isotopes knowns & expectations

.- Both systems are Borromean

Fig. from Prog. Part. Nucl. Phys. 67 (2012)939-994.  
T. Frederico et al.



# Introduction: $^{6,8}\text{He}$ isotopes knowns & expectations

.- Both systems are Borromean

.- Has the same r.m.s matter radii

Nucleus	$R_n$ (fm)	$R_p$ (fm)	$R$ (fm)
$^4\text{He}$	1.63 (0.03)	1.63 (0.03)	1.63 (0.03)
$^6\text{He}$	2.59 (0.04)	1.72 (0.04)	2.33 (0.04)
$^8\text{He}$	2.69 (0.04)	1.76 (0.03)	2.49 (0.03)

RMS radius for neutrons, protons and total

.- Comparison of cross sections, and in particular elastic scattering will not be affected by the size of the projectile

.- Thicker neutron layer of  $^8\text{He}$  may lead to weaker dipole coupling to the continuum than in the case of  $^6\text{He}$

# Introduction: $^{6,8}\text{He}$ isotopes knowns & expectations

.- Both systems are Borromean

.- Has the same r.m.s matter radii

Nucleus	$R_n$ (fm)	$R_p$ (fm)	$R$ (fm)
$^4\text{He}$	1.63 (0.03)	1.63 (0.03)	1.63 (0.03)
$^6\text{He}$	2.59 (0.04)	1.72 (0.04)	2.33 (0.04)
$^8\text{He}$	2.69 (0.04)	1.76 (0.03)	2.49 (0.03)

RMS radius for neutrons, protons and total

.- Both weakly bound

Nucleus	$S_{1n}$ (keV)	$S_{2n}$ (keV)
$^6\text{He}$	1710.0 (20)	974.8 (4)
$^8\text{He}$	2529.0 (8)	2125.8 (5)

1n and 2n energy separation

.- Comparison of cross sections, and in particular elastic scattering will not be affected by the size of the projectile

.- Thicker neutron layer of  $^8\text{He}$  may lead to weaker dipole coupling to the continuum than in the case of  $^6\text{He}$

.- Long range absorption when colliding with a heavy target at barrier energies

.-  $^8\text{He}$  is more bound

.- Breakup in  $^8\text{He} <$  breakup in  $^6\text{He}$

# Introduction: ${}^6,8\text{He}$ isotopes knowns & expectations

.- Both systems are Borromean

.- Has the same r.m.s matter radii

Nucleus	$R_n$ (fm)	$R_p$ (fm)	$R$ (fm)
${}^4\text{He}$	1.63 (0.03)	1.63 (0.03)	1.63 (0.03)
${}^6\text{He}$	2.59 (0.04)	1.72 (0.04)	2.33 (0.04)
${}^8\text{He}$	2.69 (0.04)	1.76 (0.03)	2.49 (0.03)

RMS radius for neutrons, protons and total

.- Both weakly bound

Nucleus	$S_{1n}$ (keV)	$S_{2n}$ (keV)
${}^6\text{He}$	1710.0 (20)	974.8 (4)
${}^8\text{He}$	2529.0 (8)	2125.8 (5)

1n and 2n energy separation

.- Comparison of cross sections, and in particular elastic scattering will not be affected by the size of the projectile

.- Thicker neutron layer of  ${}^8\text{He}$  may lead to weaker dipole coupling to the continuum than in the case of  ${}^6\text{He}$

.- Long range absorption when colliding with a heavy target at barrier energies

.-  ${}^8\text{He}$  is more bound

.- Breakup in  ${}^8\text{He} <$  breakup in  ${}^6\text{He}$

# Introduction: $^{6,8}\text{He}$ isotopes knowns & expectations

.-  $^{6,8}\text{He}$  1n and 2n-stripping in collisions with  $^{208}\text{Pb}$

	Q(MeV) 1n-stripping	Q(MeV) 2n-stripping
$^6\text{He}$	2.07	8.15
$^8\text{He}$	1.35	6.98

Better Q-matching for the case of  $^8\text{He}$

.- Spectroscopic factors

$$\langle ^6\text{He} | ^5\text{He} + n \rangle \sim 1.6$$

$$\langle ^8\text{He} | ^7\text{He} + n \rangle \sim 2.9$$

$$\langle ^6\text{He} | ^4\text{He} + 2n \rangle \sim \langle ^8\text{He} | ^6\text{He} + 2n \rangle \sim 1$$

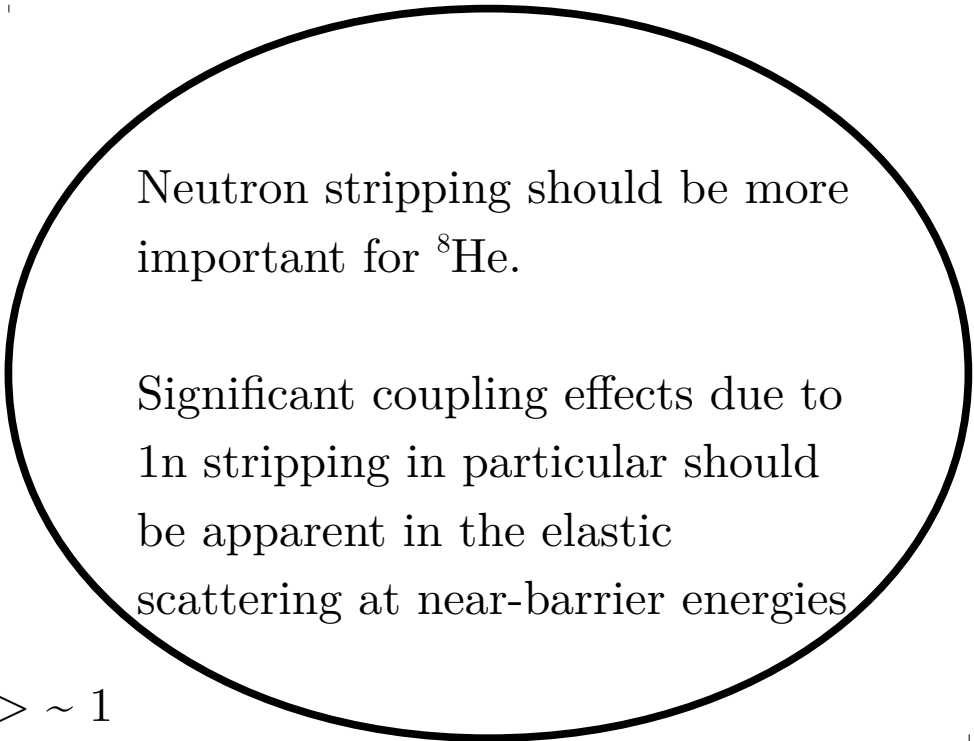


# Introduction: $^{6,8}\text{He}$ isotopes knowns & expectations

.-  $^{6,8}\text{He}$  1n and 2n-stripping in collisions with  $^{208}\text{Pb}$

	Q(MeV) 1n-stripping	Q(MeV) 2n-stripping
$^6\text{He}$	2.07	8.15
$^8\text{He}$	1.35	6.98

Better Q-matching for the case of  $^8\text{He}$



.- Spectroscopic factors

$$\langle ^6\text{He} | ^5\text{He} + n \rangle \sim 1.6$$

$$\langle ^8\text{He} | ^7\text{He} + n \rangle \sim 2.9$$

$$\langle ^6\text{He} | ^4\text{He} + 2n \rangle \sim \langle ^8\text{He} | ^6\text{He} + 2n \rangle \sim 1$$

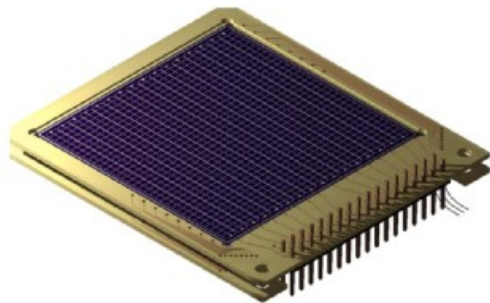


# E587S @ GANIL experimental setup

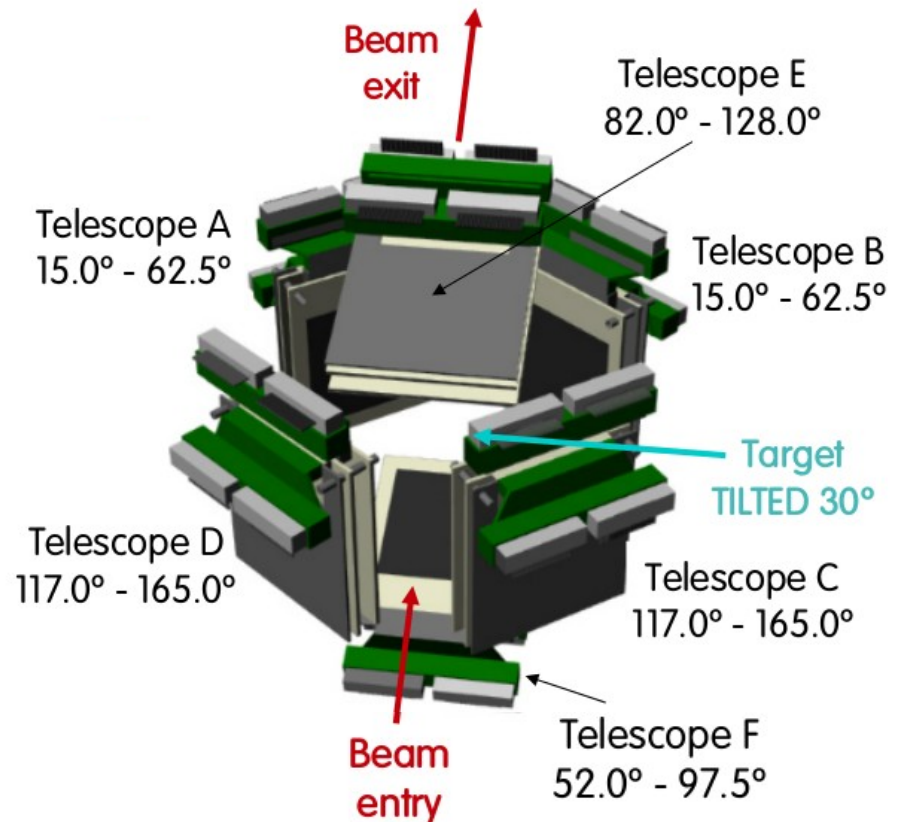
Detection system developed as part of this work with the aim of studying the structure and dynamics of exotic nuclei using nuclear reactions.

## Design requirements:

- \* Symmetric position of telescopes
- \* Maximum angular range
- \* Angular range overlap
- \* Large solid angle

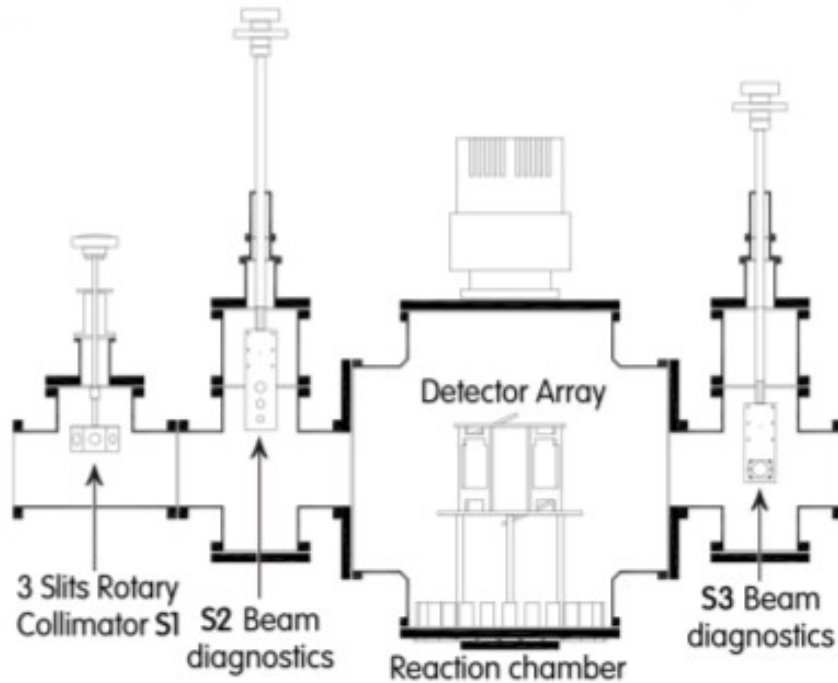


*O. Tengblad et al., Nucl. Instr. and Meth.  
Phys. Res. A525 (2004) 458.*



12 DSSD detectors arranged in 6 particle telescopes  
First stage ( $\Delta E$ ) 40  $\mu\text{m}$ , Second stage (E) 1 mm  
Total solid angle for the system: 26% ( $4\pi$ )

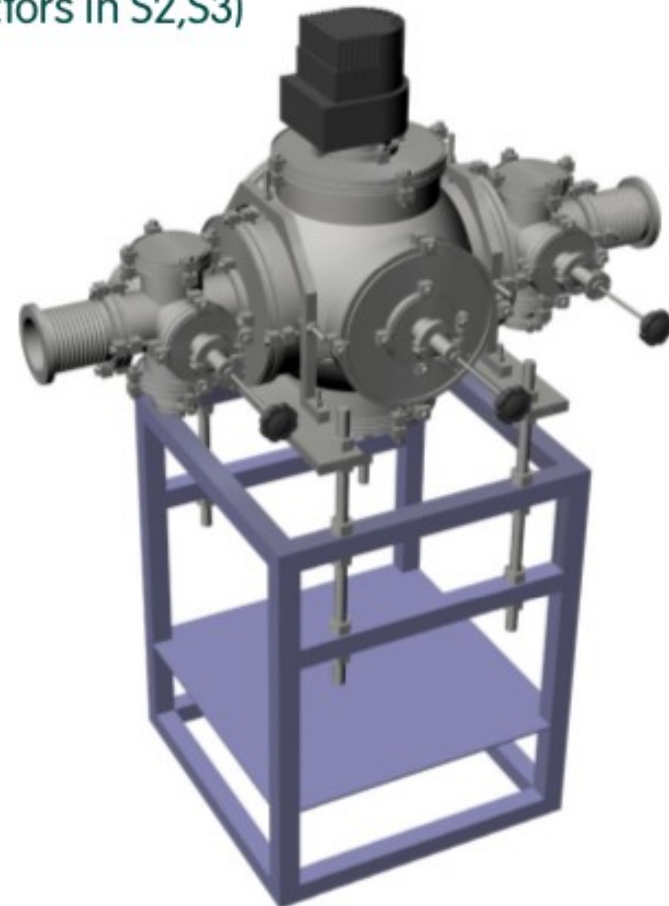
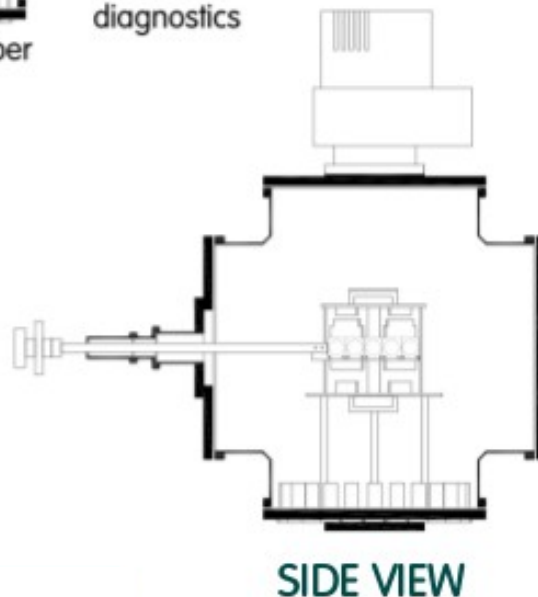
# E587S @ GANIL beam diagnostics



- \* Reaction chamber  $250\text{Ø}$  LF ( $10^{-7}$  mbar)
- \* Collimator and diagnostic systems → optimize transmission and focusing on target
- \* S1, S2 and S3 → frame with several circular collimating holes (+ faraday cup in and PIP detectors in S2,S3)

## TARGET HOLDER:

- \* Linear movement
- \* Rotatory movement



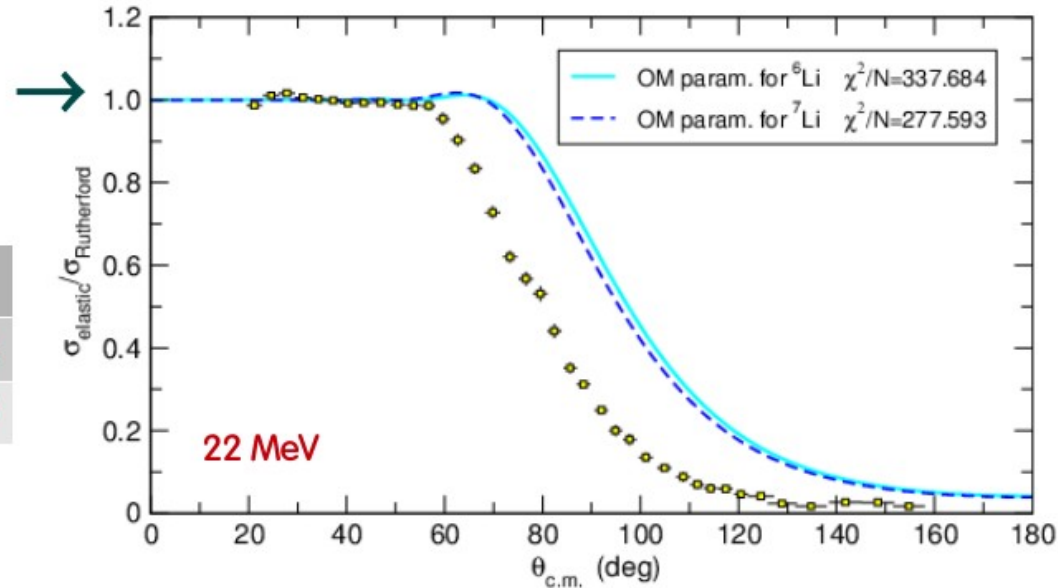
# Absorption of elastic flux

${}^8\text{He} + {}^{208}\text{Pb}$  @  $E_{\text{Lab}} = 22 \text{ MeV}$

Comparison with previous phenomenological potentials for  ${}^6,7\text{Li}$  (*J. Cook, Nucl. Phys. A388 (1982) 153*)

	$V_o$	$r_R$	$a_R$	$W_o$	$r_I$	$a_I$
${}^6\text{Li}$	109.5	1.326	0.811	22.4	1.534	0.884
${}^7\text{Li}$	114.2	1.286	0.853	9.4	1.739	0.809

$$V(r) = \frac{-V_o}{1 + \exp\left(\frac{r - r_R}{a_R}\right)} \quad W(r) = \frac{-W_o}{1 + \exp\left(\frac{r - r_I}{a_I}\right)}$$



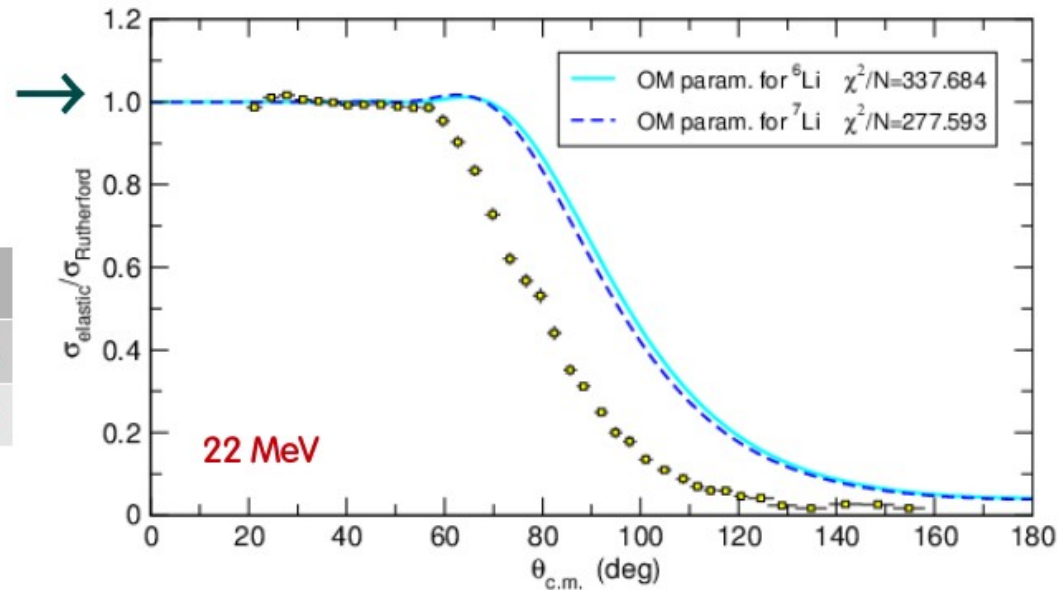
# Absorption of elastic flux

$^8\text{He} + ^{208}\text{Pb}$  @  $E_{\text{Lab}} = 22 \text{ MeV}$

Comparison with previous phenomenological potentials for  $^6,7\text{Li}$  (*J. Cook, Nucl. Phys. A388 (1982) 153*)

	$V_o$	$r_R$	$a_R$	$W_o$	$r_I$	$a_I$
$^6\text{Li}$	109.5	1.326	0.811	22.4	1.534	0.884
$^7\text{Li}$	114.2	1.286	0.853	9.4	1.739	0.809

$$V(r) = \frac{-V_o}{1 + \exp\left(\frac{r - r_R}{a_R}\right)} \quad W(r) = \frac{-W_o}{1 + \exp\left(\frac{r - r_I}{a_I}\right)}$$

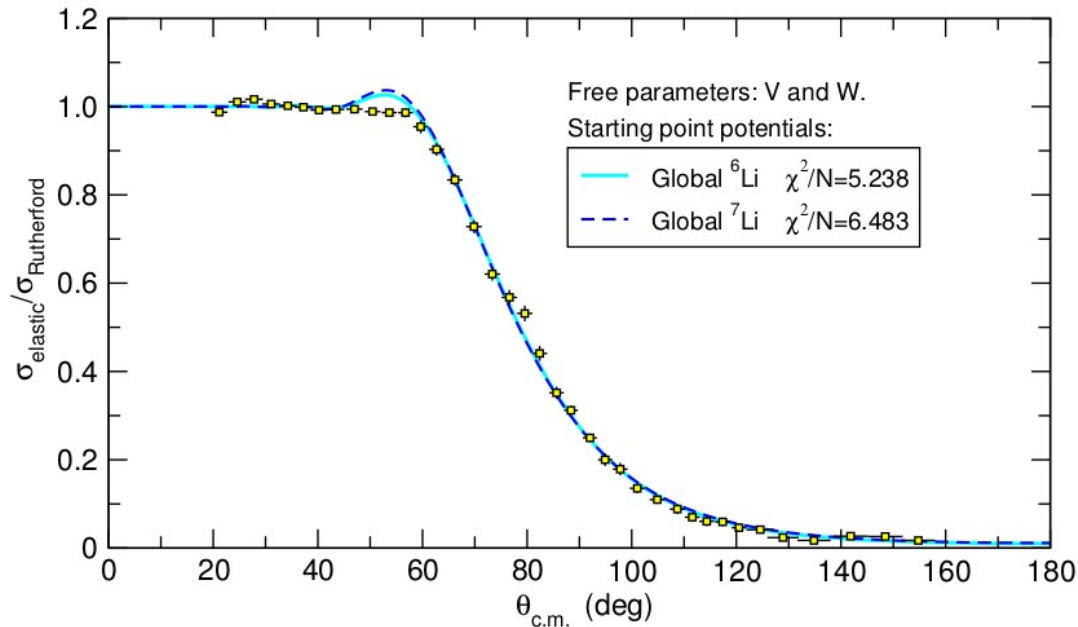


Systematics from stable nuclei do not reproduce data of  $^8\text{He}$



# Absorption of elastic flux

$^8\text{He} + ^{208}\text{Pb}$  @  $E_{\text{Lab}} = 22 \text{ MeV}$



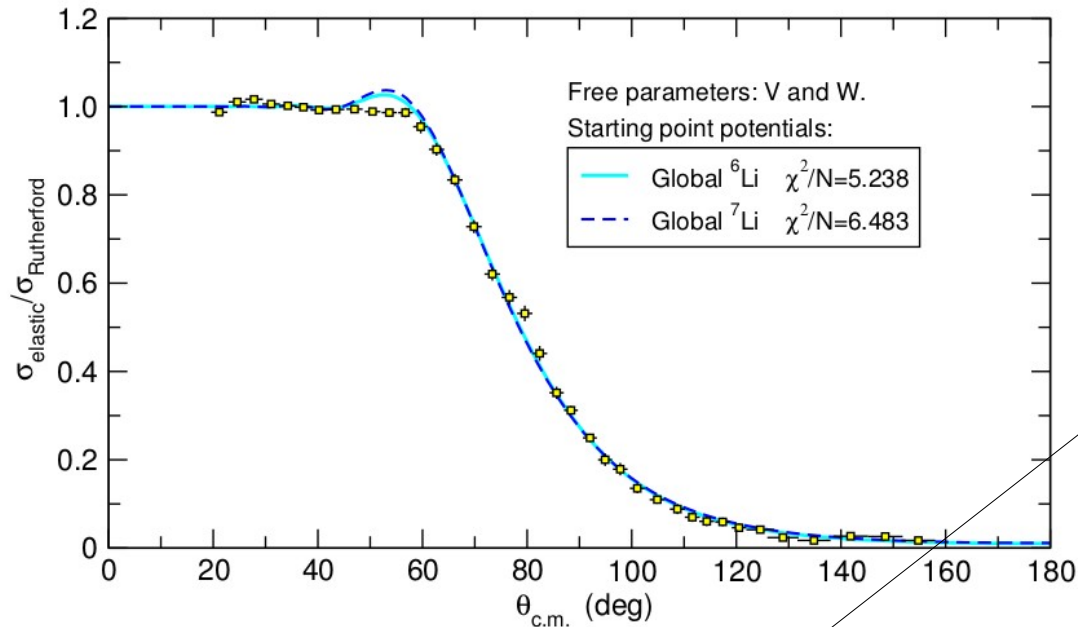
Fit with the same geometry  
(V, W free)

Starting point	V (MeV)	W (MeV)	$\chi^2 / N$
$^6\text{Li}$ global parameters	337.26	118.15	5.24
$^7\text{Li}$ global parameters	366.58	45.55	6.48

	$V_0$	$r_R$	$a_R$	$W_0$	$r_I$	$a_I$
$^6\text{Li}$	109.5	1.326	0.811	22.4	1.534	0.884
$^7\text{Li}$	114.2	1.286	0.853	9.4	1.739	0.809

# Absorption of elastic flux

$^8\text{He} + ^{208}\text{Pb}$  @  $E_{\text{Lab}} = 22 \text{ MeV}$



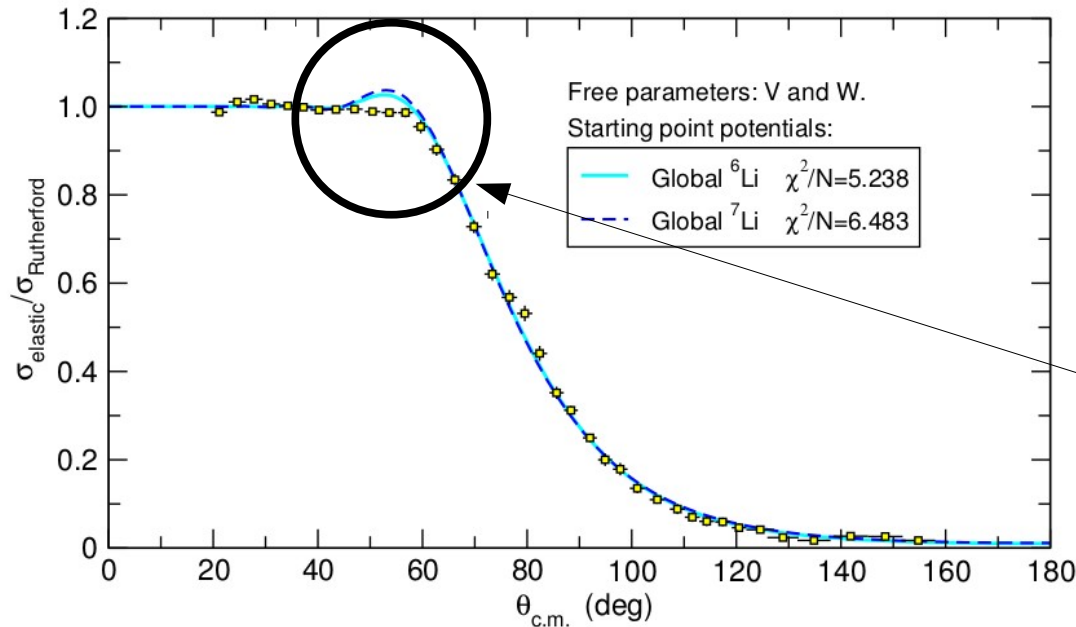
Fit with the same geometry  
( $V$ ,  $W$  free)  
- More absorption

Starting point	$V$ (MeV)	$W$ (MeV)	$\chi^2 / N$
$^6\text{Li}$ global parameters	337.26	118.15	5.24
$^7\text{Li}$ global parameters	366.58	45.55	6.48

	$V_0$	$r_R$	$a_R$	$W_0$	$r_I$	$a_I$
$^6\text{Li}$	109.5	1.326	0.81	22.4	1.534	0.884
$^7\text{Li}$	114.2	1.286	0.853	9.4	1.739	0.809

# Absorption of elastic flux

${}^8\text{He} + {}^{208}\text{Pb}$  @  $E_{\text{Lab}} = 22 \text{ MeV}$



Fit with the same geometry  
( $V$ ,  $W$  free)

- More absorption

- Still rainbow

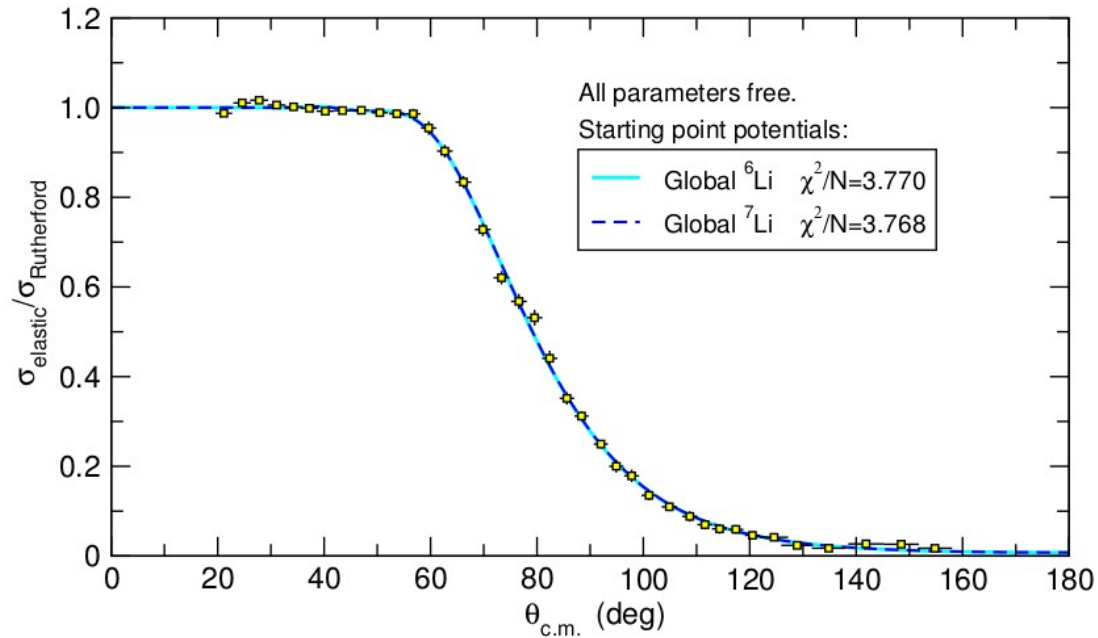
Starting point	$V$ (MeV)	$W$ (MeV)	$\chi^2 / N$
${}^6\text{Li}$ global parameters	337.26	118.15	5.24
${}^7\text{Li}$ global parameters	366.58	45.55	6.48

	$V_0$	$r_R$	$a_R$	$W_0$	$r_I$	$a_I$
${}^6\text{Li}$	109.5	1.326	0.811	22.4	1.534	0.884
${}^7\text{Li}$	114.2	1.286	0.853	9.4	1.739	0.809



# Absorption of elastic flux

$^8\text{He} + ^{208}\text{Pb}$  @  $E_{\text{Lab}} = 22$  MeV

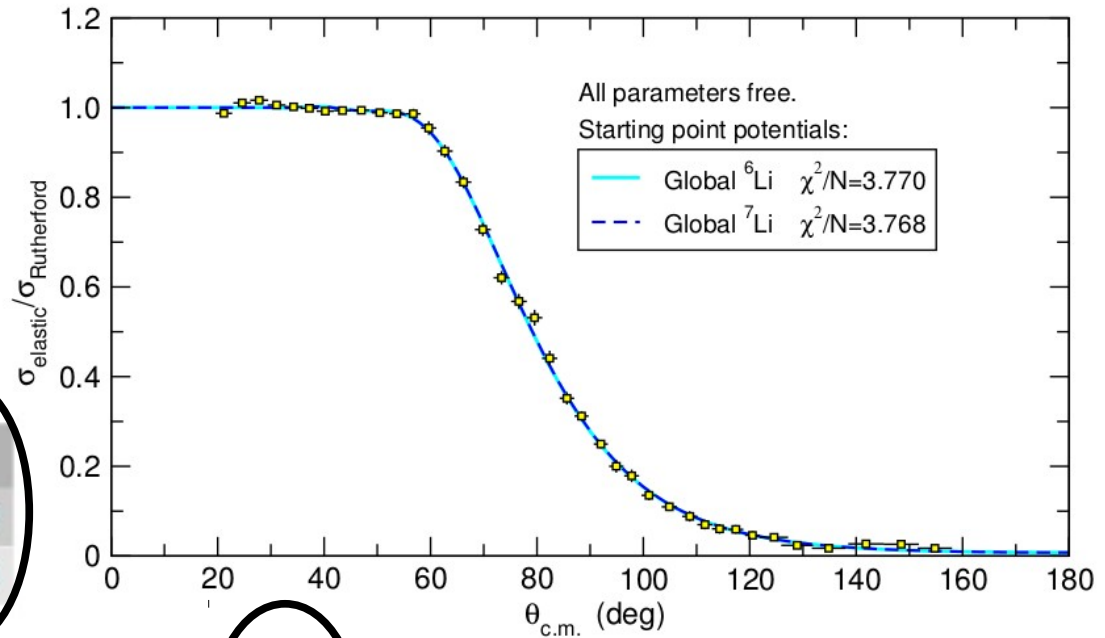


Starting point	$V$	$r_R$	$a_R$	$W$	$r_I$	$a_I$	$\chi^2/N$
$^6\text{Li}$ global	109.78	1.667	0.577	22.51	1.581	1.144	3.77
$^7\text{Li}$ global	113.46	1.657	0.583	33.51	1.501	1.147	3.77

Fit with six parameter free

# Absorption of elastic flux

$^8\text{He} + ^{208}\text{Pb}$  @  $E_{\text{Lab}} = 22 \text{ MeV}$



	$V_o$	$r_R$	$a_R$	$W_o$	$r_I$	$a_I$
$^6\text{Li}$	109.5	1.326	0.811	22.4	1.534	0.884
$^7\text{Li}$	114.2	1.286	0.853	9.4	1.739	0.809

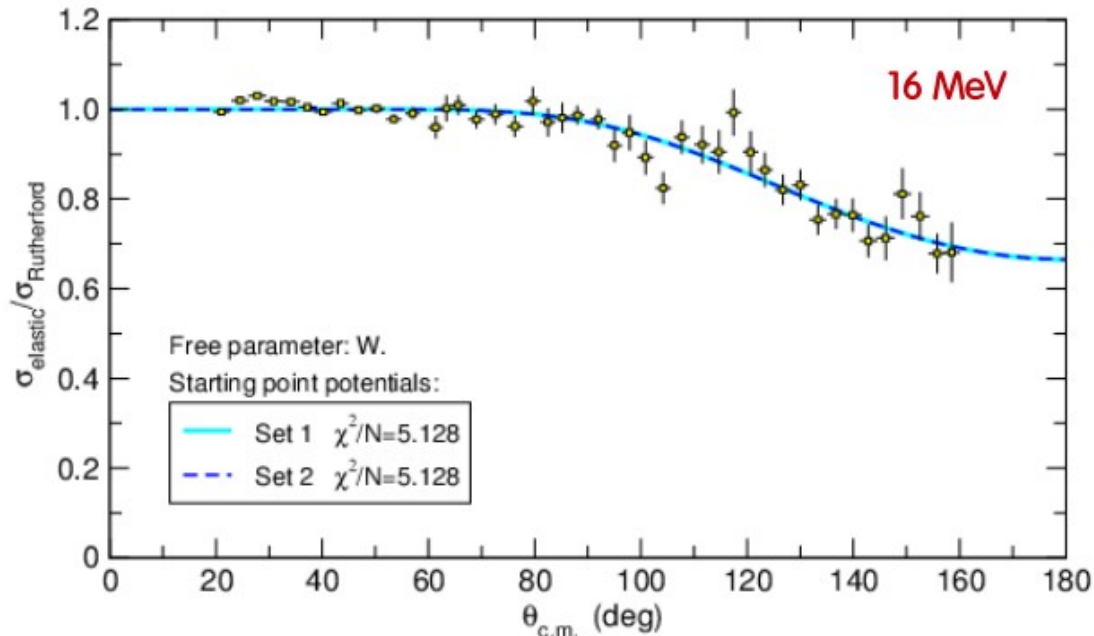
Starting point	$V$	$r_R$	$a_R$	$W$	$r_I$	$a_I$	$\chi^2/N$
$^6\text{Li}$ global	109.78	1.667	0.577	22.51	1.581	1.144	3.77
$^7\text{Li}$ global	113.46	1.657	0.583	33.51	1.501	1.147	3.77

Larger values for the imaginary diffusenesses, responsible for the absorption of flux from the elastic channel:

- \* Existence of long-range mechanisms
- \* Vanishing of the Coulomb-nuclear rainbow

# Absorption of elastic flux

${}^8\text{He} + {}^{208}\text{Pb}$  @  $E_{\text{Lab}} = 16$  MeV



Geometry of the potentials fixed for 22 MeV  $\rightarrow$  Search on  $V$  and  $W$  for 16 MeV

	$V_o$	$r_R$	$a_R$	$W_o$	$r_l$	$a_l$
${}^6\text{Li}$ global	109.8	1.667	0.577	29.7	1.581	1.144
${}^7\text{Li}$ global	113.5	1.657	0.583	44.2	1.501	1.147

$W$	
22.51	@ 22 MeV
33.51	

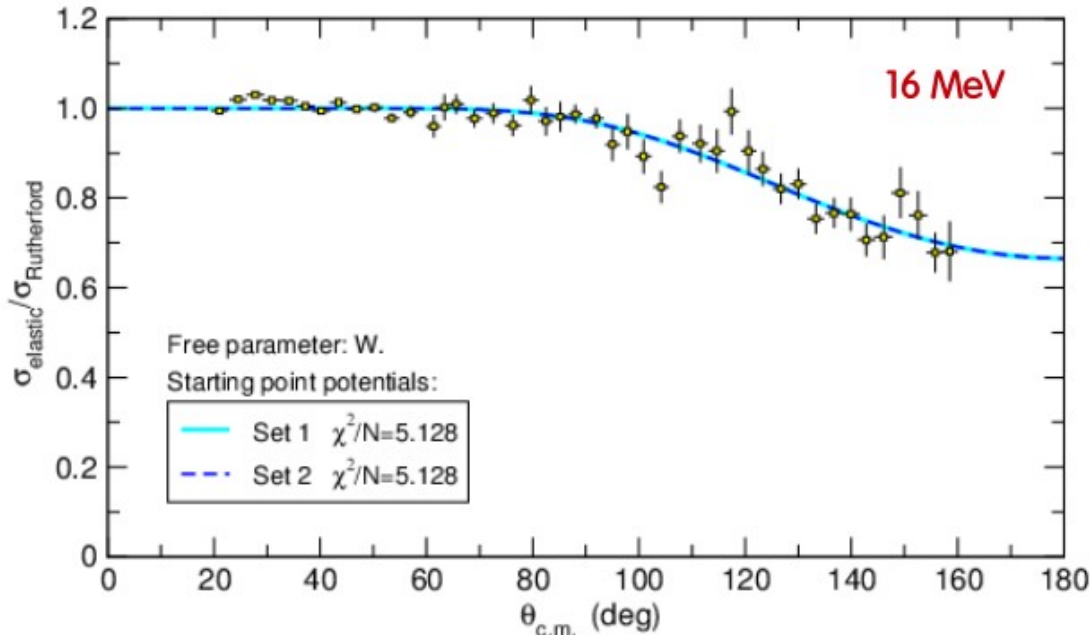
Unlike  ${}^6\text{He}$  in *A.M. Sánchez-Benítez et al.*,  $\rightarrow W(16 \text{ MeV}) > W(22 \text{ MeV}) \rightarrow$  already observed for  ${}^6\text{Li}$  in

*Nucl. Phys. A803 (2008) 30*

*N. Keeley et al., Nucl. Phys. A571 (1994) 326.*

# Absorption of elastic flux

$^8\text{He} + ^{208}\text{Pb}$  @  $E_{\text{Lab}} = 16 \text{ MeV}$



Might be due to breakup effects still present at sub-barrier energies??

Geometry of the potentials fixed for 22 MeV → Search on  $V$  and  $W$  for 16 MeV

	$V_o$	$r_R$	$a_R$	$W_o$	$r_l$	$a_l$
$^6\text{Li}$ global	109.8	1.667	0.577	29.7	1.581	1.144
$^7\text{Li}$ global	113.5	1.657	0.583	44.2	1.501	1.147

$W$	@ 22 MeV
22.51	
33.51	

Unlike  $^6\text{He}$  in *A.M. Sánchez-Benítez et al.*, →  $W(16 \text{ MeV}) > W(22 \text{ MeV})$  → already observed for  $^6\text{Li}$  in

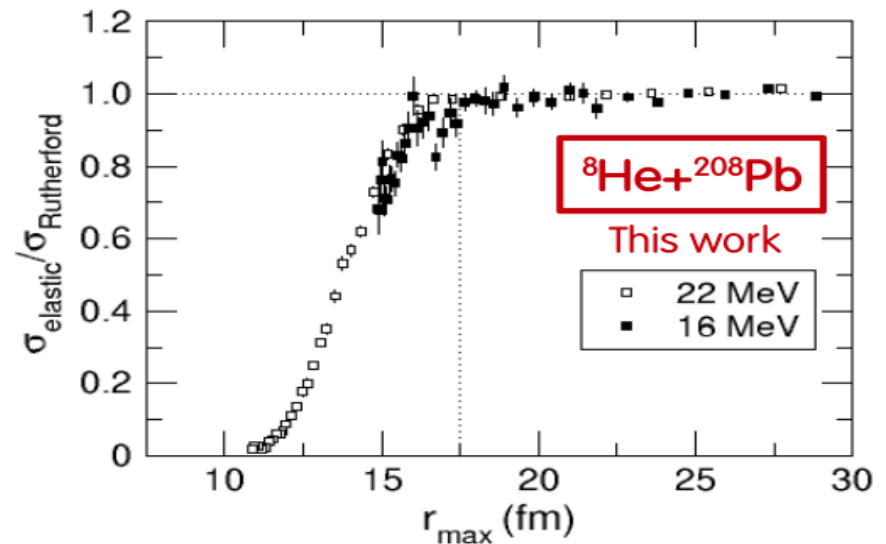
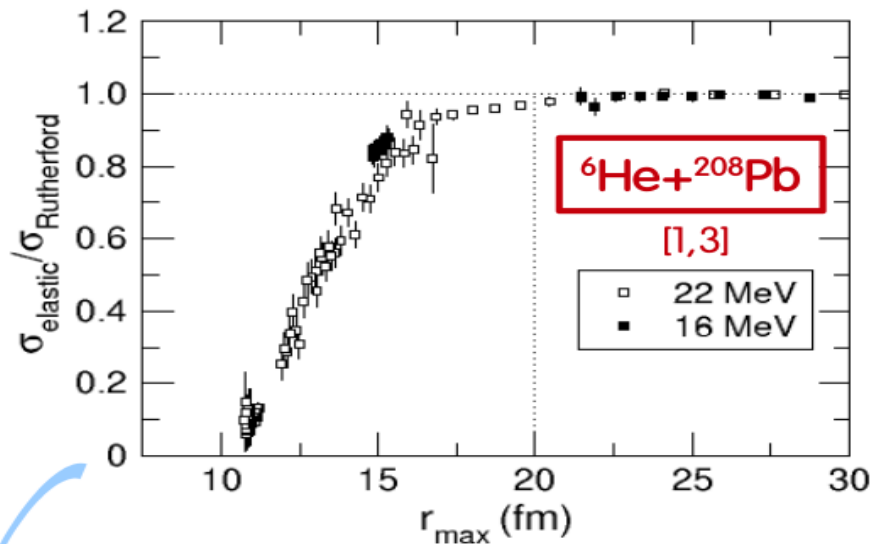
*Nucl. Phys. A803 (2008) 30*

*N. Keeley et al., Nucl. Phys. A571 (1994) 326.*

# Absorption of elastic flux in ${}^6,8\text{He}$ : range of distances

$a_i \text{ } {}^8\text{He}$  ( $\sim 1.2 \text{ fm}$ )  $\left\{ \begin{array}{l} > \text{stable nuclei} \\ < \text{halo } {}^6\text{He} (a_i = 1.89 \text{ fm}) \end{array} \right.$

$\rightarrow$  Behaviour of  ${}^6\text{He}$  will differ from Rutherford at distances  $> {}^8\text{He}$



[1] A.M. Sánchez-Benítez et al., Nucl. Phys. A803 (2008) 30  
[3] L. Acosta et al., Phys. Rev. C84 (2011)044604

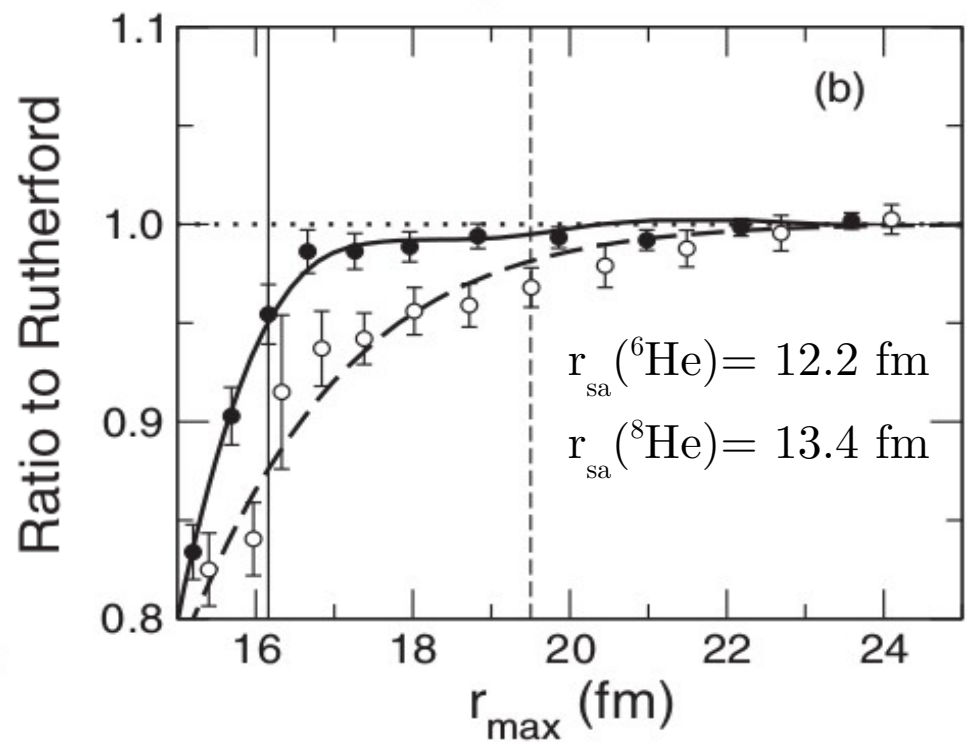
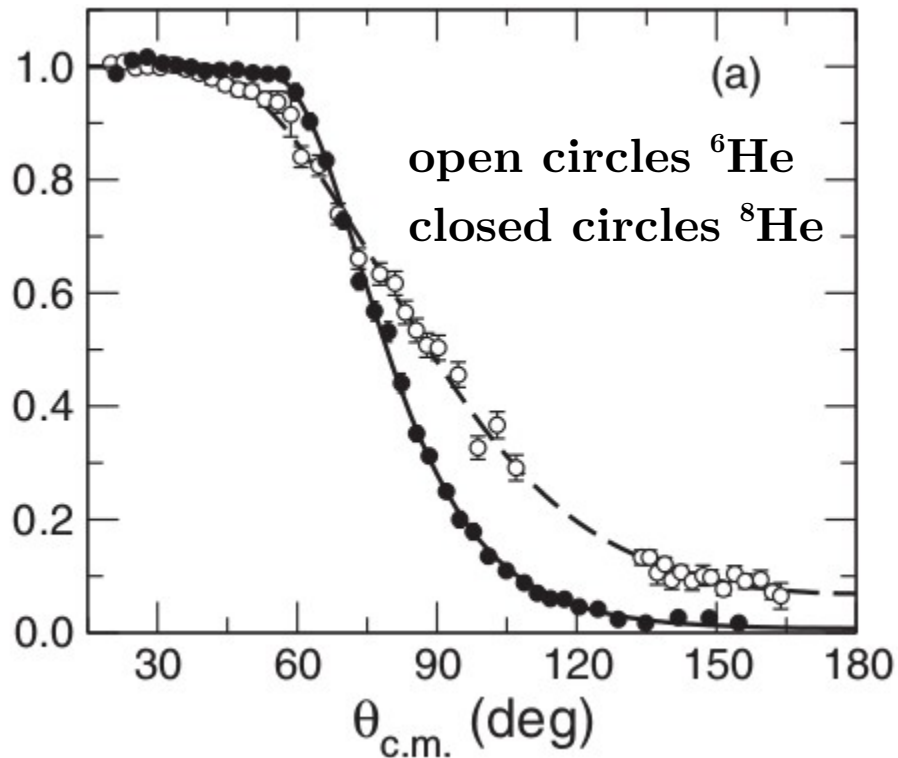
$$r_{\text{max}} = \frac{d_o}{2} \left( 1 + \frac{1}{\sin(\theta/2)} \right) \quad d_o: \text{head-on collision}$$

Common trend for various energies:  
“universal function” describing elastic scattering

$\rightarrow$  Systematic behaviour  
also found for  ${}^8\text{He}$

# Absorption of elastic flux in $^{6,8}\text{He}$ : range of distances

$^{6,8}\text{He} + ^{208}\text{Pb}$  @  $E_{\text{Lab}} = 22 \text{ MeV}$



PRC 94(2016)064618 G. Marquínez-Durán et al.

Due to highly accurate measurements:

Model independent confirmation of absorption in  $^6\text{He}$  occurs at larger distances than for  $^8\text{He}$

$r_{\text{max}}$ : distance of closest approach in a classical Coulomb trajectory

# Neutron stripping in ${}^6\text{He}$ and ${}^8\text{He}$

PRC 94(2016)064618 G. Marquínez-Durán et al.

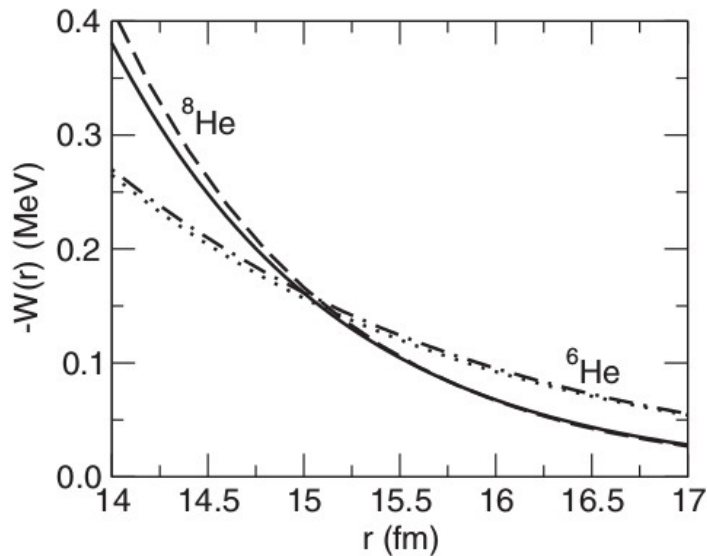


TABLE I. Optical model parameters fitting the 22 MeV  ${}^8\text{He}$  and  ${}^6\text{He} + {}^{208}\text{Pb}$  elastic scattering data. Radii follow the convention  $R_i = r_i \times A_t^{1/3}$  fm and  $r_C = 1.3$  fm.

Projectile	$V$	$r_V$	$a_V$	$W$	$r_W$	$a_W$	$\sigma_R$ (mb)	$\chi^2/N$
${}^8\text{He}$	157.1	1.651	0.557	10.5	1.733	1.137	1520	3.76
${}^6\text{He}$	114.2	1.286	0.632	9.44	1.247	1.865	1459	0.91

${}^{6,8}\text{He} + {}^{208}\text{Pb}$  @ 22 MeV

.-  $W({}^6\text{He})$  less absorptive than  $W({}^8\text{He})$

$$\sigma_R({}^6\text{He}) < \sigma_R({}^8\text{He})$$

.-  $W({}^6\text{He})$  more diffuse than  $W({}^8\text{He})$

Coul. breakup ( ${}^6\text{He}$ ) > Coul. breakup ( ${}^8\text{He}$ )

.-  $\sigma_{\text{fus}}({}^6\text{He}) \sim \sigma_{\text{fus}}({}^8\text{He})$  (fusion)



# Neutron stripping in ${}^6\text{He}$ and ${}^8\text{He}$

PRC 94(2016)064618 G. Marquínez-Durán et al.

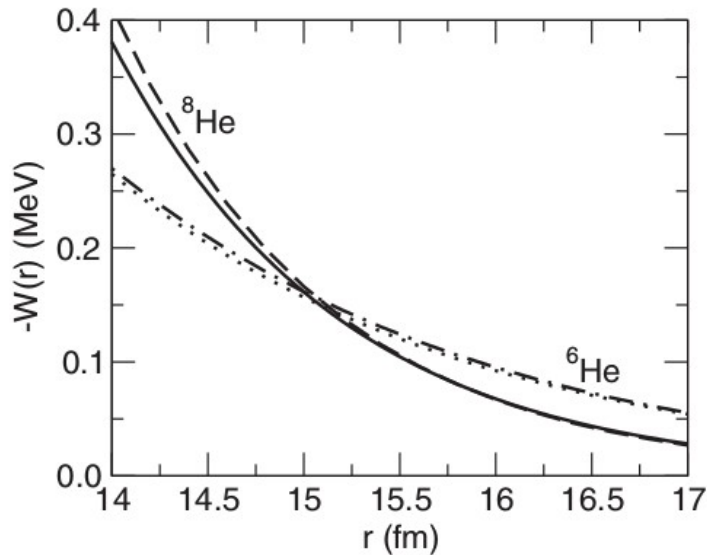


TABLE I. Optical model parameters fitting the 22 MeV  ${}^8\text{He}$  and  ${}^6\text{He} + {}^{208}\text{Pb}$  elastic scattering data. Radii follow the convention  $R_i = r_i \times A_t^{1/3}$  fm and  $r_C = 1.3$  fm.

Projectile	$V$	$r_V$	$a_V$	$W$	$r_W$	$a_W$	$\sigma_R$ (mb)	$\chi^2/N$
${}^8\text{He}$	157.1	1.651	0.557	10.5	1.733	1.137	1520	3.76
${}^6\text{He}$	114.2	1.286	0.632	9.44	1.247	1.865	1459	0.91

${}^{6,8}\text{He} + {}^{208}\text{Pb}$  @ 22 MeV

.-  $W({}^6\text{He})$  less absorptive than  $W({}^8\text{He})$

$$\sigma_R({}^6\text{He}) < \sigma_R({}^8\text{He})$$

.-  $W({}^6\text{He})$  more diffuse than  $W({}^8\text{He})$

Coul. breakup ( ${}^6\text{He}$ ) > Coul. breakup ( ${}^8\text{He}$ )

.-  $\sigma_{\text{fus}}({}^6\text{He}) \sim \sigma_{\text{fus}}({}^8\text{He})$  (fusion)

In collisions  ${}^{6,8}\text{He} + {}^{208}\text{Pb}$   
at barrier energies

(~ 20 MeV)

Neutron stripping

${}^8\text{He} \gg {}^6\text{He}$

# Summary and outlook

- The experiment E587S to study the elastic scattering and reaction channels of  ${}^6,8\text{He}+{}^{208}\text{Pb}$  @ 16, 22 MeV, below and around the Coulomb barrier, was successfully performed in GANIL.
- The detector GLORIA was used for the first time with a radioactive beam, showing excellent performances in terms of portability, energy resolution and particle identification.
- Due to the high quality of the elastic data, it is apparent in a model independent basis that absorption mechanisms takes place at longer distances for  ${}^6\text{He}$  than  ${}^8\text{He}$ .
- In the framework of the Optical Model, the previous point is confirmed and the resulting reaction cross sections suggest the neutron stripping mechanism to be stronger in the case of  ${}^8\text{He}$ .
- Angular distribution for the ratio  ${}^6\text{He}/{}^8\text{He}$  and  ${}^4\text{He}/{}^8\text{He}$  are to be interpreted in the context of breakup and neutron stripping but the structure of  ${}^8\text{He}$  makes the calculation complex.

Link to Gloria Marquínez Durán's PhD. dissertation

<http://rabida.uhu.es/dspace/handle/10272/12397>

ARIAS MONTANO REPOSITORY @ Univ. of Huelva

PUBLIC ACCESS !!

**Thank you for  
your attention !!**